

Title	Fermi-dirac and random carrier distributions in quantum dot lasers
Authors	Hutchings, M.;O'Driscoll, Ian;Smowton, P. M.;Blood, P.
Publication date	2014
Original Citation	Hutchings, M., O'Driscoll, I., Smowton, P. M. and Blood, P. (2014) 'Fermi-dirac and random carrier distributions in quantum dot lasers', Applied Physics Letters, 104(3), pp. 031103. doi: 10.1063/1.4862813
Type of publication	Article (peer-reviewed)
Link to publisher's version	<a href="http://aip.scitation.org/doi/abs/10.1063/1.4862813">http://aip.scitation.org/doi/abs/10.1063/1.4862813</a> - 10.1063/1.4862813
Rights	© 2014 AIP Publishing LLC.This article may be downloaded for personal use only. Any other use requires prior permission of the author and AIP Publishing. The following article appeared in Hutchings, M., O'Driscoll, I., Smowton, P. M. and Blood, P. (2014) 'Fermi-dirac and random carrier distributions in quantum dot lasers', Applied Physics Letters, 104(3), pp. 031103 and may be found at <a href="http://aip.scitation.org/doi/abs/10.1063/1.4862813">http://aip.scitation.org/doi/abs/10.1063/1.4862813</a>
Download date	2023-05-05 05:02:22
Item downloaded from	<a href="http://hdl.handle.net/10468/4262">http://hdl.handle.net/10468/4262</a>

## Fermi-dirac and random carrier distributions in quantum dot lasers

M. Hutchings<sup>\*</sup>, I. O'Driscoll, P. M. Snowton, and P. Blood

Citation: *Appl. Phys. Lett.* **104**, 031103 (2014); doi: 10.1063/1.4862813

View online: <http://dx.doi.org/10.1063/1.4862813>

View Table of Contents: <http://aip.scitation.org/toc/apl/104/3>

Published by the [American Institute of Physics](#)

---

---



# Fermi-dirac and random carrier distributions in quantum dot lasers

M. Hutchings,<sup>1,a)</sup> I. O'Driscoll,<sup>2,3</sup> P. M. Smowton,<sup>1</sup> and P. Blood<sup>1</sup>

<sup>1</sup>*School of Physics and Astronomy, Cardiff University, Queens Buildings, the Parade, Cardiff CF243AA, United Kingdom*

<sup>2</sup>*Tyndall National Institute, Lee Maltings, Cork, Ireland*

<sup>3</sup>*CAPPA, Cork Institute of Technology, Cork, Ireland*

(Received 4 November 2013; accepted 7 January 2014; published online 21 January 2014)

Using experimental gain and emission measurements as functions of temperature, a method is described to characterise the carrier distribution of radiative states in a quantum dot (QD) laser structure in terms of a temperature. This method is independent of the form of the inhomogeneous dot distribution. A thermal distribution at the lattice temperature is found between 200 and 300 K. Below 200 K the characteristic temperature exceeds the lattice temperature and the distribution becomes random below about 60 K. This enables the temperature range for which Fermi-Dirac statistics are applicable in QD laser threshold calculations to be identified. © 2014 AIP Publishing LLC.

[<http://dx.doi.org/10.1063/1.4862813>]

Although quantum dot (QD) lasers can have low threshold current densities ( $10.4 \text{ A cm}^{-2}$  (Ref. 1)) and high operating temperature ( $220^\circ\text{C CW}^2$ ), they have not yet fulfilled their full potential in a number of applications. This is due to several factors, many of which originate in the inhomogeneous size distribution. In particular, the temperature dependence of threshold current arises from the thermal spread of carriers across the distribution of confined energy states. It is thought that at room temperature equilibrium is achieved between the spatially separated dot states by thermal exchange of carriers with the wetting layer. However, this is not always true<sup>3</sup> and at lower temperatures dot states are occupied randomly, independent of their energy.<sup>4</sup> This has a profound influence on the temperature dependence of threshold current.<sup>5</sup> It has recently been demonstrated that random occupation in QD systems can improve mode locked laser performance where pulse widths as short as 290 fs were observed from a QD sample at 20 K, believed to be operating in the random regime.<sup>6</sup> The evidence for random occupancy on the dots was provided by fitting model calculations to the radiative threshold current of the laser. Dual wavelength lasing is currently of particular interest<sup>7</sup> due to its applications including terahertz generation,<sup>8</sup> but at present the carrier competition between the QD states is considered to be a significant limiting factor. Carrier competition between states of quantum dash lasers have been reported at room temperature,<sup>9</sup> this being ascribed to the existence of a non-equilibrium carrier distribution. Understanding and predicting the carrier distribution is a key factor in these applications.

Traditionally, the carrier temperature has been measured as the slope of a plot of the logarithm of the emission rate versus the reciprocal of photon energy at high energy. This is particularly appropriate for quantum wells where the density of states in a sub-band is insensitive to energy. However, this approach cannot be used for dots because of

the energy dependence of the number of dot states across the inhomogeneous distribution. Here, we report a method for characterising the carrier distribution across QD states from the ratio of modal gain and spontaneous emission spectra, measured by the variable stripe length method,<sup>10</sup> thereby eliminating the energy variation of the number of states. The ratio of modal gain and spontaneous emission gives a quantity  $P_m$  as a function of photon energy which is proportional to the inversion factor,  $P_F$ <sup>9</sup> which in thermal equilibrium<sup>11</sup> is

$$P_m = C \left[ 1 - \exp\left(\frac{h\nu - \Delta E_F}{k_B T}\right) \right], \quad (1)$$

where  $T$  is the temperature and  $\Delta E_F$  is the quasi-Fermi level separation of the states participating in a transition at photon energy  $h\nu$ . Equation (1) can be rearranged and written in a more general form

$$\ln[1 - P_m(h\nu)] = \frac{1}{kT_{em}}(h\nu) - \left(\frac{E^*}{kT_{em}}\right). \quad (2)$$

From this, a logarithmic plot of  $[1 - P_m]$  versus  $h\nu$  is linear if all states participating in transitions across the observed spectrum have occupation probabilities which are in quasi-equilibrium with each other at some temperature ( $T_{em}$ ) determined from the slope of this plot.  $T_{em}$  is a property of the gain and emission spectra and arises from the energy distributions of the electrons and holes which participate in these transitions. This may not be the same as the temperature of the lattice ( $T_L$ ). The intercept of the plot gives a value for  $E^*$  which is a measure of the energy separation of the groups of populated electron and holes states participating in the transitions. In quasi-equilibrium this is the quasi-Fermi level separation. Departures from quasi-equilibrium are indicated by non-linear plots of  $\ln[1 - P_m(h\nu)]$ , or linearity over a limited range of photon energy, and by values of  $T_{em}$  which do not correspond to those expected for quasi-equilibrium distributions of electrons and/or holes at the lattice temperature. The purpose of this paper is to present results for  $T_{em}$  as a

<sup>a)</sup>Present address: Author now working in the Physics Department at Syracuse University, Physics Building, Syracuse, NY, 13244, USA. E-mail: mdhutc01@syr.edu.

function of lattice temperature for a quantum dot laser sample and to discuss their interpretation.

We use the following three phrases to describe the nature of the carrier occupation within the measured QD sample.

- **Thermal occupancy:** The  $\ln[1-P_m(h\nu)]$  plots are linear with a slope which gives  $T_{em}$  equivalent to  $T_L$ . (In quasi-equilibrium  $T_{em}$  and  $T_L$  are not equal for reasons discussed below.) The QD and wetting layer states are in thermal equilibrium with the lattice and occupation of all states can be described by global Fermi-Dirac electron and hole distributions.
- **Quasi-thermal occupancy:** The energy dependence of  $\ln[1-P_m(h\nu)]$  is linear, can be fitted by Eq. (2), and is therefore Fermi Dirac in form, but  $T_{em}$  is not equivalent to  $T_L$ . The dot states have an internal quasi-equilibrium but are not in equilibrium with the lattice.
- **Random Occupancy:** The value of  $T_{em}$  is very much greater than the lattice temperature, indicative of a very flat distribution in energy. Although the occupation probability is independent of the energy of the dot states in the random regime the infinite value of  $T_{em}$  which this implies is not measured, the explanation for this is given below.

We have studied a  $1.3\ \mu\text{m}$  laser structure grown by molecular beam epitaxy (MBE). The active region consist of five layers of InAs dots each grown in a dot-in-a-well (DWELL) consisting of  $\text{In}_{0.15}\text{Ga}_{0.85}\text{As}$  and surrounded by a GaAs core and  $\text{Al}_{0.45}\text{Ga}_{0.55}\text{As}$  cladding layer. The wafer was fabricated into  $50\ \mu\text{m}$  wide oxide-insulated stripe segmented contact devices with  $300\ \mu\text{m}$  long sections for measurement of modal gain and spontaneous emission spectra by the multi section technique<sup>10</sup> between 25 K and 300 K using a 0.05% duty cycle pulsed electrical injection.

From these measurements, logarithmic plots of  $[1-P(h\nu)]$  versus photon energy were constructed as in Eq. (2) and examples made over a range of injection levels at 300 K are shown in Figure 1.

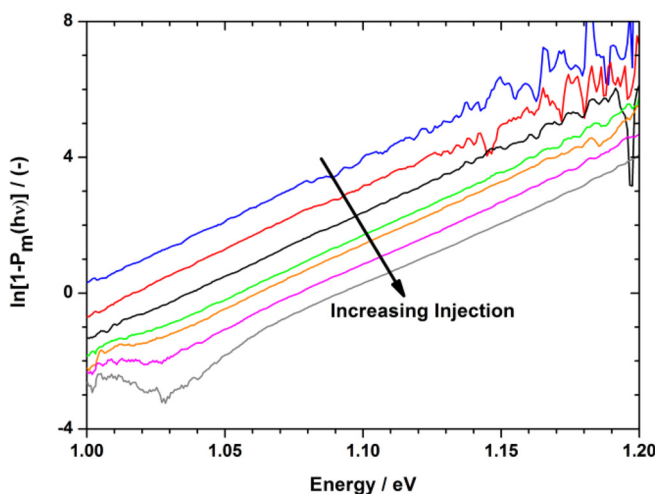


FIG. 1. Logarithmic plots of  $[1-P(h\nu)]$  versus photon energy for the undoped sample at measured at 300 K for current densities of  $50\ \text{Acm}^{-2}$ ,  $83.3\ \text{Acm}^{-2}$ ,  $133.3\ \text{Acm}^{-2}$ ,  $200\ \text{Acm}^{-2}$ ,  $233.3\ \text{Acm}^{-2}$ ,  $333.3\ \text{Acm}^{-2}$ ,  $466.7\ \text{Acm}^{-2}$ .

The energy range in Figure 1 covers the ground and excited state inhomogeneous distributions. The plots are linear with similar gradients, with the highest and lowest current densities shown giving  $T_{em}$  values of  $(322 \pm 5)\ \text{K}$  and  $(316 \pm 10)\ \text{K}$ , respectively. The linearity of the plots suggest that the occupation within QD states themselves can be described by Fermi-Dirac statistics, thus a single  $T_{em}$  can be defined at each injection level, and that there is no discernible dependence of  $T_{em}$  on injection at this temperature. These plots give an average  $T_{em}$  of  $(325 \pm 10)\ \text{K}$  which is different to the lattice temperature (300 K).

Equation (1) assumes that at any photon energy there is only one transition between a single pair of states, however this is not the case in the presence of homogeneous broadening (HB), or overlapping ground and excited state distributions. To examine the effect of the former, we have modelled an inhomogeneous distribution of dots occupied according to Fermi-Dirac statistics at the lattice temperature and subject to HB. The inhomogeneous distribution was matched to that of the sample by fitting the calculated absorption spectrum to the measured absorption obtained in real units using multi section technique.<sup>10</sup> We used a temperature dependent linewidth<sup>12</sup> to produce modal gain and emission spectra from which logarithmic  $[1-P_m]$  plots were simulated. At 300 K  $T_{em} = 326\ \text{K}$  was obtained from these calculations and this is consistent with our measured  $T_{em}$ . The effect of homogeneous broadening is to “flatten” the spectra giving an apparently higher  $T_{em}$  from the QD states and we conclude that at 300 K the dot occupation can be described by a Fermi function with  $T_L = 300\ \text{K}$  across ground and excited states.

At all measured lattice temperatures the logarithmic plots of  $[1-P_m]$  were linear so the emission spectra can each be characterised by a single temperature. Figure 2 shows the  $T_{em}$  values extracted from the measurements made on the sample between 25 K and 300 K. The data is plotted for fixed levels of modal gain between  $8\ \text{cm}^{-1}$  and  $20\ \text{cm}^{-1}$  at each  $T_L$ . The  $T_{em}$  extracted between 25 K and 300 K from the

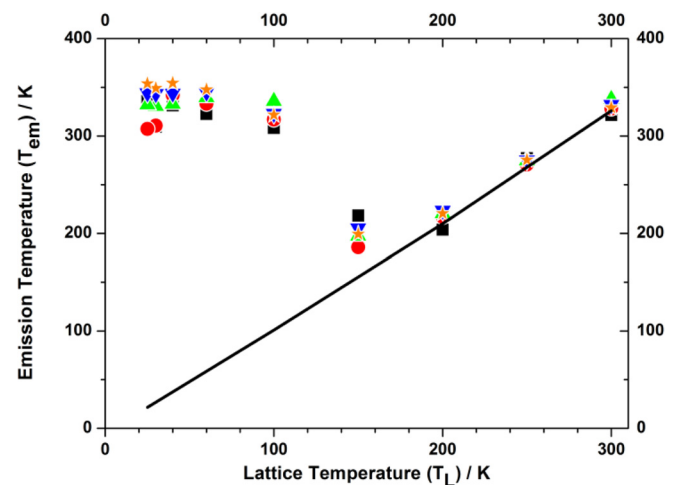


FIG. 2. Emission temperature ( $T_{em}$ ) at fixed modal gains of  $8\ \text{cm}^{-1}$  (squares),  $10\ \text{cm}^{-1}$  (circles),  $12\ \text{cm}^{-1}$  (Up triangles),  $16\ \text{cm}^{-1}$  (down triangles), and  $20\ \text{cm}^{-1}$  (stars) plotted against lattice temperature ( $T_L$ ) for the undoped sample. Also plotted is  $T_{em}$  calculated from the Fermi-Dirac model of the QD ensemble including HB (solid black line).

model Fermi Dirac calculations described above is also included on Figure 2 as a continuous line.

In Figure 2, we observe excellent quantitative agreement between the measured  $T_{em}$  and those calculated from the model between 200 K and 300 K with the difference between  $T_{em}$  and  $T_L$  being due to homogeneous broadening of the emission. Therefore, it can be concluded that the QD states are in thermal equilibrium with the wetting layer and the lattice between 200 K and 300 K.

At a  $T_L$  of 150 K,  $T_{em}$  is measured to be  $(200 \pm 15)$  K. This is significantly greater than  $T_L$  and indicates that the occupied dot states are not in thermal equilibrium with the lattice and the carriers have a wider energy spread than that corresponding to the lattice temperature. The transition to quasi-thermal occupancy agrees with measurements on similar samples showing a minimum in radiative and threshold current density at 200 K, attributed to this transition.<sup>3</sup>

As  $T_L$  is decreased from 150 K down to 25 K,  $T_{em}$  increases before a plateau is reached at a  $T_L$  of 60 K and below, where  $T_{em} = (340 \pm 15)$  K. The fact that  $T_{em}$  is independent of  $T_L$  in this region suggests the dot occupation is oblivious to the lattice temperature, as occurs with random population. However, if the occupation of QD states was truly random, the probability of occupancy would be totally independent of energy and  $P_m$  would have a constant value. This would result in the logarithmic plot of  $[1-P(h\nu)]$  being flat giving an infinite measured value for  $T_{em}$ .

To fully understand the behaviour of  $T_{em}$  at 60 K and below all recombination, relaxation and excitation processes occurring within the QD and wetting layer states of this sample must be considered. Figure 3 illustrates of two possible state population models that might occur within any given QD sample. In both cases radiative ( $\tau_{rad}$ ) (red solid arrows) and phonon induced ( $B_{ph}$ ) (black dashed arrows) processes are indicated.

Model (a) in Figure 3 includes phonon-induced transitions of electrons between the wetting layer and the QD excited states (ES) and between the wetting layer and QD ground states (GS) as well as radiative recombination from those QD states. If these ESs and GSs are then populated randomly from the wetting layer the occupation would be totally independent of energy across ground and excited states and would lead to an infinite  $T_{em}$ . Model (b) in Figure 3 includes the phonon-induced exchange of carriers between the ESs and GSs within the same dot. In a random population case the ES and GS are still occupied individually independently of energy, however, any carrier captured into the ES of a dot can relax into the GS of that same dot. In the random regime there is no upward thermal emission and the occupation is given by

$$f = \frac{1}{1 + \frac{\tau_{in}}{\tau_{out}}}, \quad (3)$$

where  $(\tau_{in})^{-1}$  is the overall rate at which electrons are gained by the state and  $(\tau_{out})^{-1}$  the overall rate at which carriers are lost. The excited state loses carriers by phonon-mediated capture to the ground state and by recombination to the hole state (small  $\tau_{out}$ , small  $f$ ), whereas the ground states only lose

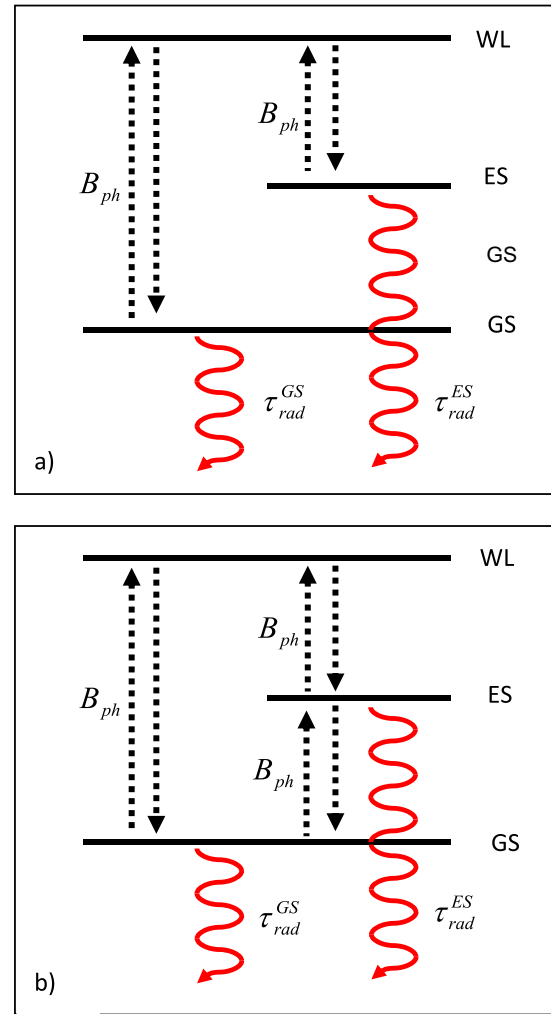


FIG. 3. An illustration of two possible state population models that might occur within any given QD sample. (a) Interaction between WL and ground and excited states of the QDs; (b) as (a) but also includes interaction between ground and excited state within each QD. Both radiative (red arrows) and non-radiative (black arrows) processes are illustrated.

carriers by recombination but gain carriers by capture from the wetting layer (WL) and from the excited state (small  $\tau_{in}$ , bigger  $f$ ). Consequently, the excited state has lower occupancy than the ground state and a different value of  $P_m$ . Since the energy range of the plots covers ground and excited states and these inhomogeneous distributions overlap, the measured  $P_m$  varies across the spectra with a gradual transition going from ground to and excited state distributions. Therefore, the measured  $P_m$  across the spectrum has an energy dependence and  $T_{em}$  is not infinite. Our measurements of  $T_{em}$  therefore show that below 60 K the dot occupation is random and that there is a “trickle-down” of electrons for the excited to ground states in individual dots.

The width of the emission spectrum from a QD sample at any given  $T_L$ , characterised through these  $T_{em}$  measurements, has a direct consequence for the temperature dependence of the radiative and threshold current density of a working device so the understanding and insight this analysis provides is of great importance. We can extract the radiative threshold current density from our measurements by calculating the area under the spontaneous emission spectra, which we obtain in real units,<sup>10</sup> and we can determine the



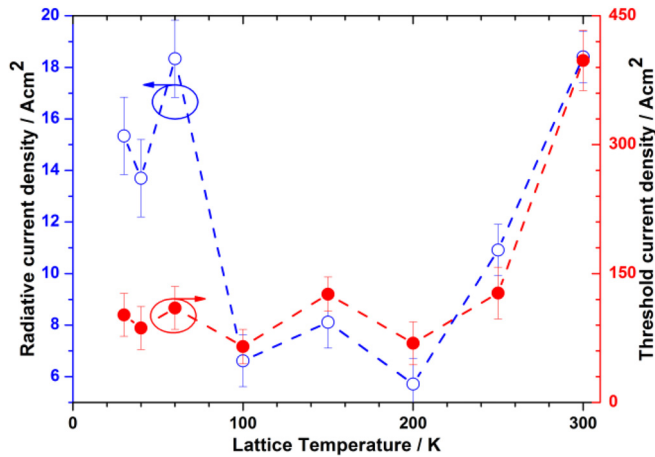


FIG. 4. Radiative (empty circles) and threshold (filled circles) current density versus temperature measured from the sample at a fixed net gain of  $6\text{ cm}^{-1}$  (2 mm laser).

total threshold current required for a given length laser by measuring the total current density required to achieve a specific peak modal gain. The radiative and total current densities at threshold versus temperature are shown for a fixed gain of  $6\text{ cm}^{-1}$  in Figure 4. This fixed net gain is the lasing requirement for a 2 mm laser.

In Figure 4 we observe that the radiative and total threshold current density measured for this sample increases monotonically between 200 K and 300 K. This is a direct result of the  $T_{em}$  for this sample where the thermal occupancy of the QD states resulted in an increase in  $T_{em}$  as the temperature of the sample is increased between 200 K and 300 K. This undesirable temperature dependence commonly limits QD laser performance around room temperature. Our  $T_{em}$  measurements have identified the temperature range over which the QD states are thermally occupied and will have a strongly temperature dependent lasing threshold. The radiative current density increases as the temperature is decreased from 100 K to 60 K and then remains constant down to 25 K. This mirrors the behaviour of the  $T_{em}$  over this temperature range so we can conclude that the increase in radiative current density occurs as the QDs become completely decoupled from the wetting layer and occupation of the QD states becomes random.

In summary, we have described a method to characterise the carrier distribution across the radiative states in a QD laser structure in terms of a temperature, using experimentally measured gain and emission spectra. This method is independent of the form of the inhomogeneous state distribution, so can be applied to any material. A thermal distribution at the lattice temperature is observed for a QD sample between 200 and 300 K. Below 200 K the characteristic temperature exceeds the lattice temperature and the distribution becomes random below about 60 K. This method of characterisation enables the temperature range for which Fermi-Dirac statistics are applicable in QD laser threshold calculations to be identified and could be relevant for micro-cavity lasers where the stimulated rate per unit area can be large. An emission temperature that is independent of variations in lattice temperature is indicative of random QD occupation so this characterisation method can determine the temperature at which thermal emission from the QD states to the wetting layer ceases. This understanding will greatly assist the development of QD devices with high temperature random QD regime operation for mode locking and dual wavelength applications.

<sup>1</sup>D. G. Deppe, K. Shavritranuruk, G. Ozgur, H. Chen, and S. Freisem, *Electron. Lett.* **45**, 54 (2009).

<sup>2</sup>T. Kageyam, K. Takada, K. Nishi, M. Yamaguchi, R. Mochida, Y. Maeda, H. Kondo, K. Takemasa, Y. Tanaka, T. Yamamoto, M. Sugawara, and Y. Arakawa, *Proc. SPIE* **8277**, 72 (2012).

<sup>3</sup>I. O'Driscoll, P. M. Smowton, and P. Blood, *IEEE J. Quantum Electron.* **45**, 380 (2009).

<sup>4</sup>M. Grundmann and D. Bimberg, *Phys. Rev. B* **55**, 9740 (1997).

<sup>5</sup>I. O'Driscoll, P. M. Smowton, and P. Blood, *J. Quantum Electron.* **46**, 525 (2010).

<sup>6</sup>P. Finch, P. Blood, P. M. Smowton, A. Sobiesierski, R. M. Gwilliam, and I. O'Driscoll, *Appl. Phys. Lett.* **103**, 131109 (2013).

<sup>7</sup>M. V. Maximov, Y. M. Shernyakov, F. I. Zubov, A. E. Zhukov, N. Yu Gordeev, V. V. Korenev, A. V. Savelyev, and D. A. Livshits, *Semicond. Sci. Technol.* **28**, 105016 (2013).

<sup>8</sup>N. A. Naderi, F. Grillot, K. Yang, J. B. Wright, A. Gin, and L. F. Lester, *Opt. Express* **18**, 27028 (2010).

<sup>9</sup>C. L. Tan, H. S. Djie, Y. Wang, C. E. Dimas, V. Hongpinyo, Y. H. Ding, and B. S. Ooi, *IEEE Photonics Technol. Lett.* **21**, 30 (2009).

<sup>10</sup>P. Blood, G. M. Lewis, P. M. Smowton, H. Summers, J. Thomson, and J. Lutt, *IEEE J. Sel. Top. Quantum Electron.* **9**, 1275 (2003).

<sup>11</sup>H. D. Summers, J. D. Thomson, P. M. Smowton, P. Blood, and M. Hopkinson, *Semicond. Sci. Technol.* **16**, 140 (2001).

<sup>12</sup>P. Borri, W. Langbein, S. Schneider, U. Woggon, R. L. Sellin, D. Ouyang, and D. Bimberg, *IEEE J. Sel. Top. Quantum Electron.* **8**, 984 (2002).